THE ASTROPHYSICAL JOURNAL, 334:657–664, 1988 November 15

IMAGES IN THE ROCKET ULTRAVIOLET: UV FLUXES OF M31 GLOBULAR CLUSTERS

RALPH C. BOHLIN
Space Telescope Science Institute

ROBERT H. CORNETT, JESSE K. HILL, AND ROBERT S. HILL
ST Systems Corporation

AND

THEODORE P. STECHER
Laboratory for Astronomy and Solar Physics, Goddard Space Flight Center
Received 1987 December 29; accepted 1988 May 10

ABSTRACT

From images obtained by a rocket-borne ultraviolet imaging telescope, near-UV ($\sim$2700 Å) fluxes are determined for 17 sources in M31 that are optical globular-cluster candidates and for the bright open cluster vdB0 (Hodge cluster 107) in M31. Far-UV ($\sim$1500 Å) fluxes or flux limits are determined for the same clusters. The resulting $m_{\rm NUV} - V$ and $m_{\rm FUV} - V$ colors are compared with those of Galactic clusters. The $m_{\rm NUV} - V$ colors for M31 clusters are similar to those of Galactic clusters, except for the high-metallicity M31 cluster Bo 171, whose observed $m_{\rm NUV} - V$ may be due to a younger age or an anomalously blue horizontal branch. Our $m_{\rm FUV} - V$ limits are not stringent enough to decide between these possibilities. Four of the detected clusters have optical, $m_{\rm NUV} - V$, and $m_{\rm FUV} - V$ colors indicating ages $\sim 10^8$ yr, which are much less than those of typical Galactic globular clusters, but which are similar to that of cluster vdB0. These four clusters are probably similar to the so-called "blue globular" clusters of the LMC. The existence of young LMC-type blue globulars and the possible existence of middle-aged metal-rich globulars may indicate that M31 has continued to form globular clusters throughout its life.

Subject headings: clusters: globular — galaxies: individual (M31) — photometry — ultraviolet: general

I. INTRODUCTION

Ultraviolet imagery is an excellent means for investigating regions of active star formation, where the emission is dominated by luminous hot massive stars (Bohlin *et al.* 1982; Hill, Bohlin, and Stecher 1984). Observations of the globular cluster M5 have shown that populations of evolved low-mass stars in UV-bright evolutionary phases can also be studied effectively by means of rocket-UV imagery (Bohlin *et al.* 1983, 1985*b*). The prominent local group SAb spiral M31 (NGC 224), containing both types of UV-emitting populations, was observed at $\sim 15''$ resolution by our rocket-borne telescope, a prototype for the Ultraviolet Imaging Telescope (UIT) to be flown on the Astro Spacelab missions (Stecher *et al.* 1984). The instrument was flown on Astrobee flight 25.053 at 7:30 UT 1980 August 8.

Bohlin *et al.* (1985*a*) reported the results of an investigation of the UV emission of the central bulge of M31, giving an upper limit on the contribution of young main sequence stars and an estimate of the contribution from horizontal-branch and hot post–AGB stars. Here, we investigate the UV fluxes of the globular cluster candidates found on optical images (Battistini *et al.* 1987). This investigation became feasible because of the acquisition and development of image processing software for UIT data processing with greatly enhanced capabilities for astrometric and photometric analysis (Cornett, Hill, and Hill 1987).

II. OBSERVATIONS

The payload consisted of a 31 cm f/5.6 Ritchey-Chretien telescope with two microchannel plate image intensifiers coupled to II-aO film (Bohlin *et al.* 1982). The wavelengths of maximum sensitivity for the two cameras were near 1400 Å (CsI cathode) and 2700 Å (CsTe cathode) with bandwidths 440 Å and 860 Å, respectively. The effective wavelength for the wide CsTe bandpass depends on the source spectrum and varies from 2380 Å for unreddened hot stars to 2740 Å for the M31 bulge, and the effective wavelength for the narrower CsI bandpass varies from 1400 Å to 1490 Å for the same sources. The field of view was 80′ in diameter with FWHM $\sim 15''$ for a point source.

Images were obtained of two overlapping fields of M31, with the nucleus and surrounding bulge regions included in both. The flight data and associated laboratory calibration frames were digitized and reduced following the general procedure described by Bohlin *et al.* (1982).

The payload was destroyed when the parachute system failed, but the damaged film cassettes were recovered. The absolute calibration was determined from the linearized and flat-fielded microdensitometry of the bulge region. The bandpass response functions of the two cameras were integrated over a spectrum interpolated from *ANS* fluxes of the same region (Wu *et al.* 1980), using the corrected *ANS* calibration of Bohlin, Harrington, and Stecher (1982). Similar treatment of short exposures gave absolute calibrations consistent with the longer exposures to within 3% for the near-UV camera, thus verifying the linearity of the reduced data.

Although most frames suffered some degradation in the crash, the data appeared to be only locally affected by enhanced background for four CsTe frames (6B, 7B, 13B, and 15B) with exposure times 12 s, 25 s, 12 s, and 20 s, and for 2 CsI frames (6A and 10A) with exposure times of 60 s. The longer-exposure images have been published as Figure 1 of Bohlin *et al.* (1985*a*). The UV emission from M31 is dominated by the bulge and by a ring of OB associations (van den Bergh 1964) and H II regions (Baade and Arp 1964; Courtès *et al.* 1978).

III. SOURCE PHOTOMETRY AND CLUSTER IDENTIFICATION

The M31 images have been searched for point sources (FWHM < 20″) using a version of DAOPHOT (Stetson 1987) modified for eventual use with UIT data (Cornett, Hill, and Hill 1987). Photometry is done both using an aperture of diameter 48″ and by fitting the PSF to source profiles using a separately determined PSF for each frame. (No evidence is found for significant PSF variation within a frame.) From the longest near-UV exposures, ~1000 sources brighter than ~17.5 mag are measurable with rms error ~0.2 mag. From the noisier far-UV frames, ~500 sources brighter than ~17.5 mag are measurable with rms error ~0.5 mag. Our UV magnitudes are defined by the usual relation $m = -2.5 \log f - 21.1$, where f is the flux in units of ergs cm^{-2} s^{-1} Å^{-1}. The internal photometric error is determined from the statistics of the magnitude differences obtained for spatially coincident sources on different frames. In addition, sources as faint as ~19 mag in the near UV and ~18 mag in the far UV can be measured by stacking individual exposures as explained below. (Note that for DAOPHOT, the limiting magnitude actually is determined locally by source crowding, so that it varies over each image.) In the following discussion, we refer to magnitudes measured from near-UV (CsTe) frames as $m_{\rm NUV}$ and to magnitudes measured from far-UV (CsI) frames as $m_{\rm FUV}$.

Identifying and measuring clusters requires three steps: (1) searching a near-UV frame for sources; (2) identifying a subset of these sources with clusters; and (3) searching the corresponding far-UV frame in the neighborhood of each cluster confirmed in the near UV. The far-UV frames have this dependent status because they are noisier than the near-UV frames.

Plate solutions are determined using astrometry software that identifies visual astrometric standards from the Space Telescope Guide Star Catalog (Lasker and McLean 1987) with detected UV sources. On each near-UV image, ~100 standard stars are identifiable, and on each far-UV image, ~25 standard stars are identifiable. Every identified standard star is used in fitting plate constants. The resulting rms positional accuracy for arbitrary sources is 5″.

The derived plate solutions allow images to be aligned with one another by resampling onto a common coordinate grid, which in this case is done by bicubic interpolation. The images are then summed for an increase in effective exposure time. This method is used to produce a summed image of the 20′ × 20′ region centered on the nucleus in each bandpass, for a total exposure time of 69 s in the near UV and 120 s in the far UV. The modified DAOPHOT program finds 735 sources brighter than ~19 mag in the summed near-UV image.

M31 cluster candidates discovered optically and cataloged by the Bologna group (Battistini *et al.* 1987) are used to identify clusters among the UV sources found by the photometry program. For the summed near-UV bulge image, a total of 16 of the 72 Bologna clusters in the field are within 7″ of UV sources. The number of chance coincidences between the list of globular clusters and the list of detected UV sources can be estimated as a function of the maximum separation that defines a coincidence, assuming positions from both lists are randomly distributed over the image. A critical distance of 7″ leads to an estimate of 4 ± 2 chance coincidences out of 72. Consistent with this estimate, three of the 16 coincidences are with clusters that are both faint and red at optical bandpasses ($B-V > 0.9$ and $V > 16.5$). Therefore the UV flux measurements at these three positions probably provide only upper limits. Figure 1 (Plate 5) shows the summed near-UV bulge image and identifies the 13 probable clusters. Limiting near-UV magnitudes ranging from 17.0 to 18.5 mag for the 56 undetected Bologna clusters are determined by adding artificial sources to the UV image at the optical position. The faintest artificial source that can be found by the photometry program is the upper limit to the UV brightness.

In the disk regions of the two longest near-UV exposures, the photometry program finds four other probable clusters, three of which are so-called "blue globulars" (§ V). Figure 2 (Plate 6) shows the SW portion of near-UV image 7B with the three disk blue globulars circled, along with vdB0 and Bo 338 (§§ IV–V).

The far-UV frames are searched for sources coinciding with cluster candidates previously identified with near-UV sources. Where no coincident source is found, a local limiting magnitude is computed in the same way as described above for the near UV.

IV. M31 GLOBULAR CLUSTERS COMPARED WITH GALACTIC CLUSTERS

M31 and the Galaxy are generally considered to be very similar SAb spirals. However, optical data on their globular cluster systems show surprising differences. The M31 clusters are described by van den Bergh (1969) as more metal rich on the average. Burstein *et al.* (1984) find the spectra of M31 clusters to show enhanced Hβ and CN absorption relative to Galactic clusters, possibly due to younger ages. Cowley and Burstein (1988) conclude on the basis of *IUE* spectra of selected bright M31 clusters that some may be as young as 2×10^9 yr. Because of the sensitivity of cluster UV colors to age, metallicity, and horizontal branch type (van Albada, Dickens, and Wevers 1981; van Albada, de Boer, and Dickens 1981), a UV comparison of the two cluster systems is of interest.

For the 17 detected Bologna clusters, Table 1 gives catalog numbers from the Battistini *et al.*; Sargent *et al.* (1977), and Vetesnik (1962) lists; $m_{\rm NUV}$ and $m_{\rm FUV}$ as measured by us; and BV measurements by van den Bergh (1969) where possible, and by Battistini *et al.* otherwise. Dereddened $m_{\rm NUV} - V$, $m_{\rm FUV} - V$, and absolute magnitude M_V are also given, calculated using the mean Galactic reddening curve (Savage and Mathis 1979). The adopted $E(B-V)$ is given for each cluster. A distance modulus of 24.07 for M31 (de Vaucouleurs 1978) is used to compute M_V. Our conclusions would not be altered significantly if we adopted a distance modulus of 24.34, as advocated by Pritchet and van den Bergh (1987).

Bo 148, Bo 151, Bo 171, and Bo 182 have $B-V > 1.0$ as measured by Battistini *et al.*, suggesting the possibility of larger values of $E(B-V)$ than can be accounted for by foreground Galactic reddening of $E(B-V) = 0.10$. However, in the case of Bo 148, we accept $E(B-V) = 0.10$ because of the lower $B-V$ of 0.80 reported by Sharov and Lyuty (1983). Bo 151, Bo 171, and Bo 182 are also observed by Frogel, Persson, and Cohen (1980), who determine $E(V-K)$ values that imply $E(B-V)$ values 0.35, 0.10, and 0.27, respectively.

The four Bologna clusters with $B-V < 0.4$ are discussed in § V, along with the final entry in Table 1, cluster vdB0 (Hodge 1979; open cluster 107). We adopt $E(B-V) = 0.2$ for all these blue clusters, as described in § V.

Figure 3 shows dereddened $m_{\rm NUV} - V$ versus M_V for the 18 detected M31 clusters from Table 1 (including vdB0) and for the 19 Galactic globular clusters observed both by van Albada, deBoer, and Dickens (1981) with *ANS* and by Kron and Mayall (1960) in the visible (with an aperture approximately equal to that of *ANS*). The limiting near-UV fluxes of the 56

1988ApJ...334..657B

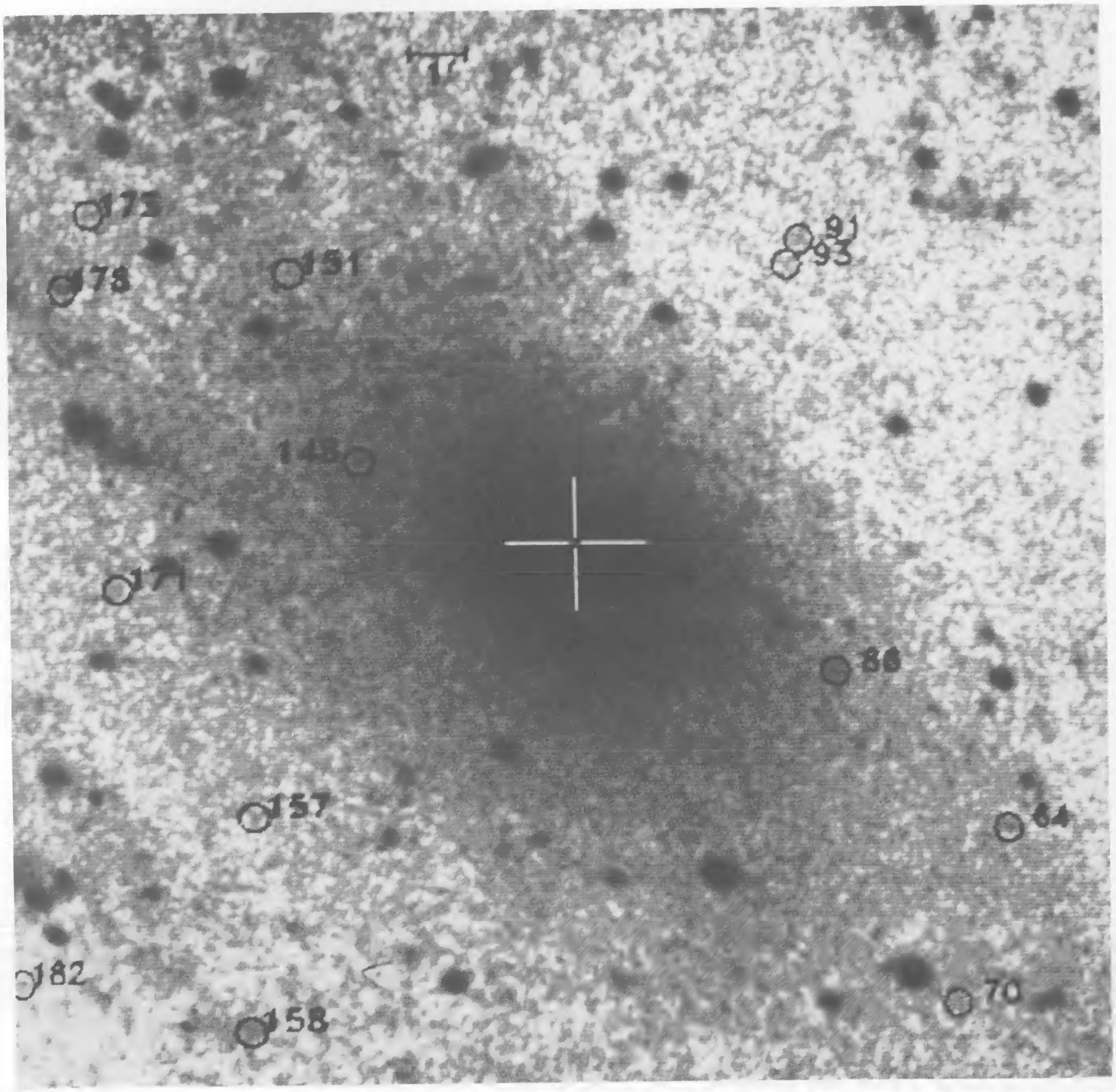

FIG. 1.—Combined near-UV M31 20′ × 20′ bulge image, with detected Bo clusters circled. The position of the center of the cross is $\alpha_{1950} = 0^h39^m59^s.7$, $\delta_{1950} = 40°59′49″$. North is at the top; east is at the left.

BOHLIN *et al.* (*see* **334**, 658)

1988ApJ...334..657B

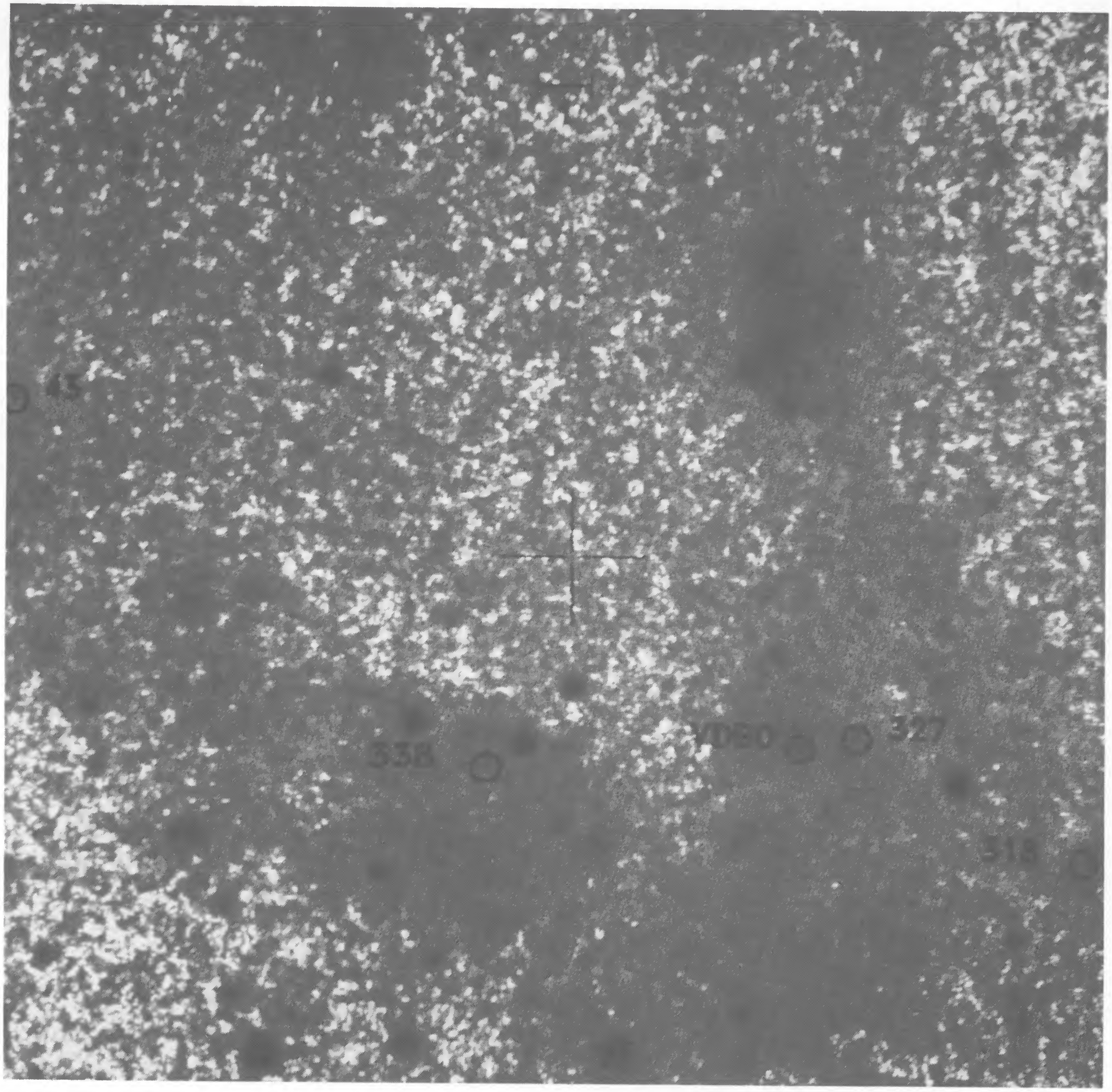

FIG. 2.—SW portion of near-UV image 7B, with three detected blue globulars (Bo 43, Bo 318, and Bo 327), vdB0, and the position of Bo 338 circled. The position of the cross is $\alpha_{1950} = 0^h38^m7^s.2$, $\delta_{1950} = 40°23'16''$. North is at the top; east is at the left.

BOHLIN *et al.* (*see* **334**, 658)

TABLE 1

CLUSTER PHOTOMETRY

Bo[a]	K[b]	Vet[c]	m_{NUV}	m_{FUV}	V	$B-V$	M_V[d]	$E(B-V)$	$m_{NUV}-V$[d]	$m_{FUV}-V$[d]
43[e]	106	21	17.3	16.5	17.01	0.23	−7.39	0.20	−0.6	−1.5
64	125	49	17.6	>18.0	16.29	0.81	−8.09	0.10	0.9	>0.4
70	133	45	18.8	>18.0	16.77	0.76	−7.61	0.10	1.6	> −0.8
86	148	62	17.3	16.3	15.05	0.85	−9.33	0.10	1.8	0.8
91[e]	151	251	17.8	>17.2	17.75	0.34	−6.94	0.20	−0.8	> −2.4
93	155	82	18.6	>18.0	16.70	0.79	−7.68	0.10	1.4	>0
148	200	86	17.8	>17.0	15.77	1.03	−8.61	0.10	1.6	>0.2
151	205	93	18.9	17.7	14.84	1.08	−10.32	0.35	2.5	1.1
157	212	72	19.3	>18.0	17.39	0.76	−6.99	0.10	1.4	> −1.6
158	213	64	17.5	>16.8	14.63	0.90	−9.75	0.10	2.5	>1.7
171	222	87	18.6	>17.0	15.27	1.08	−9.11	0.10	2.9	>1.0
173	224	264	18.8	>17.6	17.51	0.85	−6.87	0.10	0.8	> −1.2
178	229	95	17.2	18.2	15.05	0.83	−9.33	0.10	1.7	>0.8
182	233	73	18.1	>16.7	15.41	1.04	−9.50	0.27	1.5	>0
206	257	106	17.2	>17.0	15.26	0.91	−9.12	0.10	1.5	>1.2
318[e]	42	7	17.2	16.4	16.97	0.23	−7.72	0.20	−0.7	−1.6
327[e]	53	...	16.9	>16.5	16.71	0.19	−7.98	0.20	−0.7	> −1.2
vdB0[e]	...	...	15.7	14.7	14.94	0.20	−9.75	0.20	−0.1	−1.2

[a] Catalog number from Battistini *et al.* 1987.
[b] Catalog number from Sargent *et al.* 1977.
[c] Catalog number from Vetesnik 1962.
[d] Dereddened as described in text.
[e] Blue as described in text.

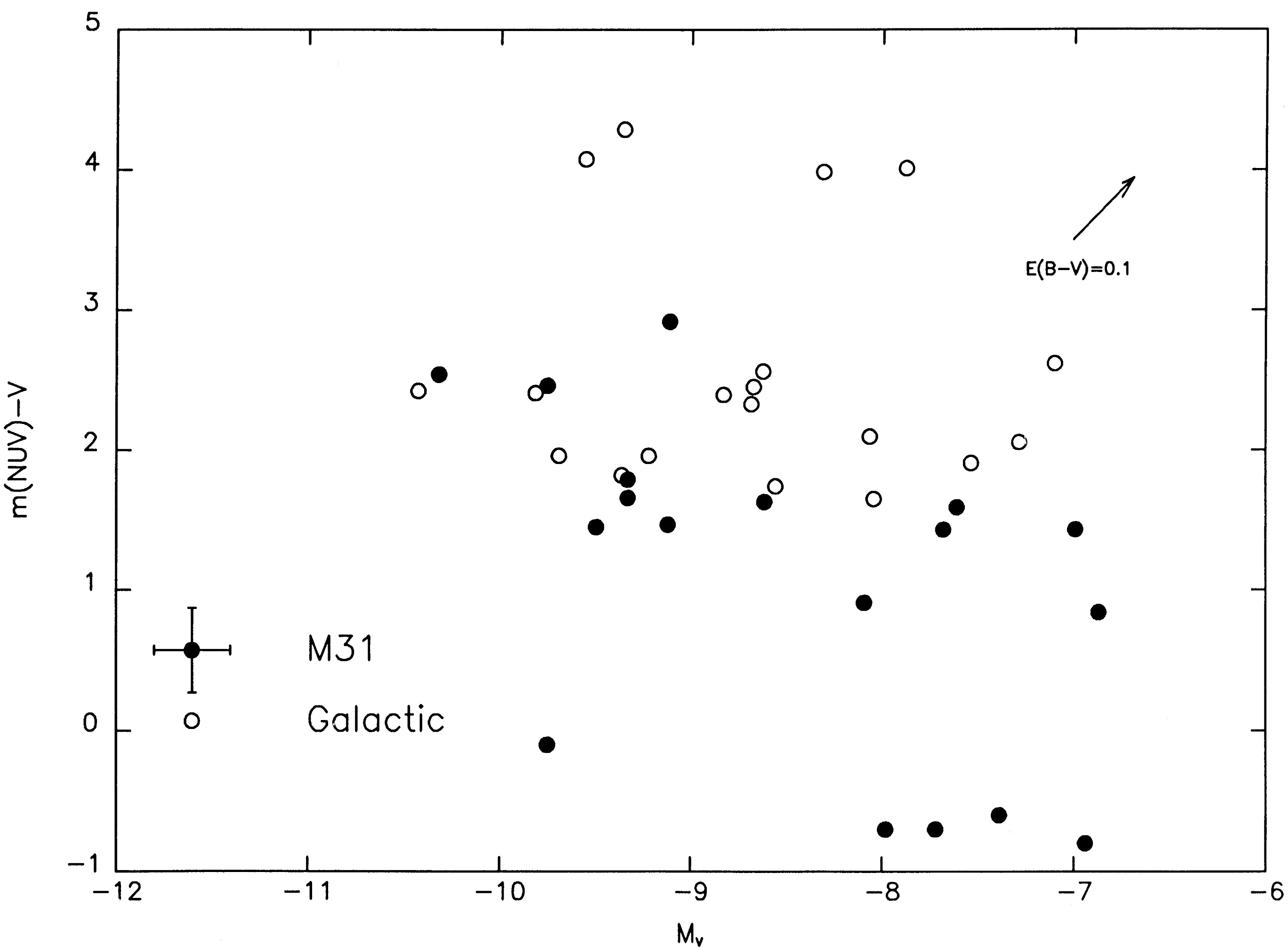

FIG. 3.—Dereddened $M_V - (m_{NUV} - V)$ diagram for M31 and Galactic globular clusters. Filled circles refer to M31 clusters with UV rocket measurements and visual photometry by Battistini *et al.* (1987). The error bar refers to the M31 cluster points. Open circles refer to Galactic clusters with *ANS* 2500 Å band measurements by van Albada, deBoer, and Dickens (1981) and visual magnitudes in an equivalent aperture from Kron and Mayall (1960). The arrow indicates how a source would be displaced in the plot if it were undercorrected for reddening by $E(B-V) = 0.1$.

undetected Bologna clusters imply limiting $m_{NUV} - V$ colors, but these points are omitted from Figure 3, as they all lie within the $m_{NUV} - V$ range of the detected clusters and are therefore uninformative. For the Galactic clusters the *ANS* 2500 Å band magnitude adjusted by +0.33 mag is used as m_{NUV}. This adjustment, which accounts for the difference between the broad near-UV band and the narrow *ANS* 2500 Å band, is computed on the basis of Kurucz (1979) model atmospheres of T_{eff} ranging from 5500 K – 6500 K.

The detected M31 clusters and the Galactic clusters occupy approximately the same region in Figure 3, except for the absence of measured M31 clusters with $m_{NUV} - V > 3.5$ and the absence of Galactic clusters with $m_{NUV} - V < 0$. If present in M31, clusters as red as the reddest Galactic clusters would have near-UV magnitudes near or beyond our detection limit. That the visually fainter clusters we detect tend to be bluer is understandable from the fact that any visually faint red clusters would be too faint in the UV for us to detect. The five M31 clusters with $m_{NUV} - V < 0.0$ are discussed in § V.

The results of van Albada, Dickens, and Wevers (1981) indicate that for the Galactic clusters $m_{NUV} - V$ is sensitive primarily to metallicity, since 0.72 of the flux in the *ANS* 2500 Å band is from main-sequence turn-off stars, even for metal-poor clusters with blue horizontal branches, which van Albada, deBoer, and Dickens (1981) call clusters of class B. For such clusters, as well as for clusters with redder horizontal branches, since $m_{NUV} - V$ is determined mainly by main-sequence turn-off stars, for lower metallicity clusters are bluer because of decreased line blanketing in the near UV. In addition, however, a dependence of $m_{NUV} - V$ on horizontal-branch type is evident for clusters with intermediate metallicities and extremely blue *ANS* colors and horizontal branches, which van Albada, deBoer, and Dickens (1981) call clusters of class EB. Figure 4 plots $m_{NUV} - V$ versus the metallicity index [Fe/H] for 13 non-EB Galactic clusters, six EB Galactic clusters, and four M31 clusters with metallicities determined from $V-K$ by Frogel, Persson, and Cohen (1980).

Figure 4 also includes points derived from Kurucz (1979) atmospheres with metallicity [Fe/H] = −2, −1, and 0, main-sequence gravities, and T_{eff} = 5500 K and 6000 K (near the main-sequence turnoff for Galactic globulars). The dependence of $m_{NUV} - V$ on line blanketing is evident, as well as the general agreement of the model-atmosphere colors with Galactic-cluster data.

The four M31 clusters plotted in Figure 4 (Bo 151, Bo 158, Bo 171, and Bo 182) occupy a region in the plot consistent with

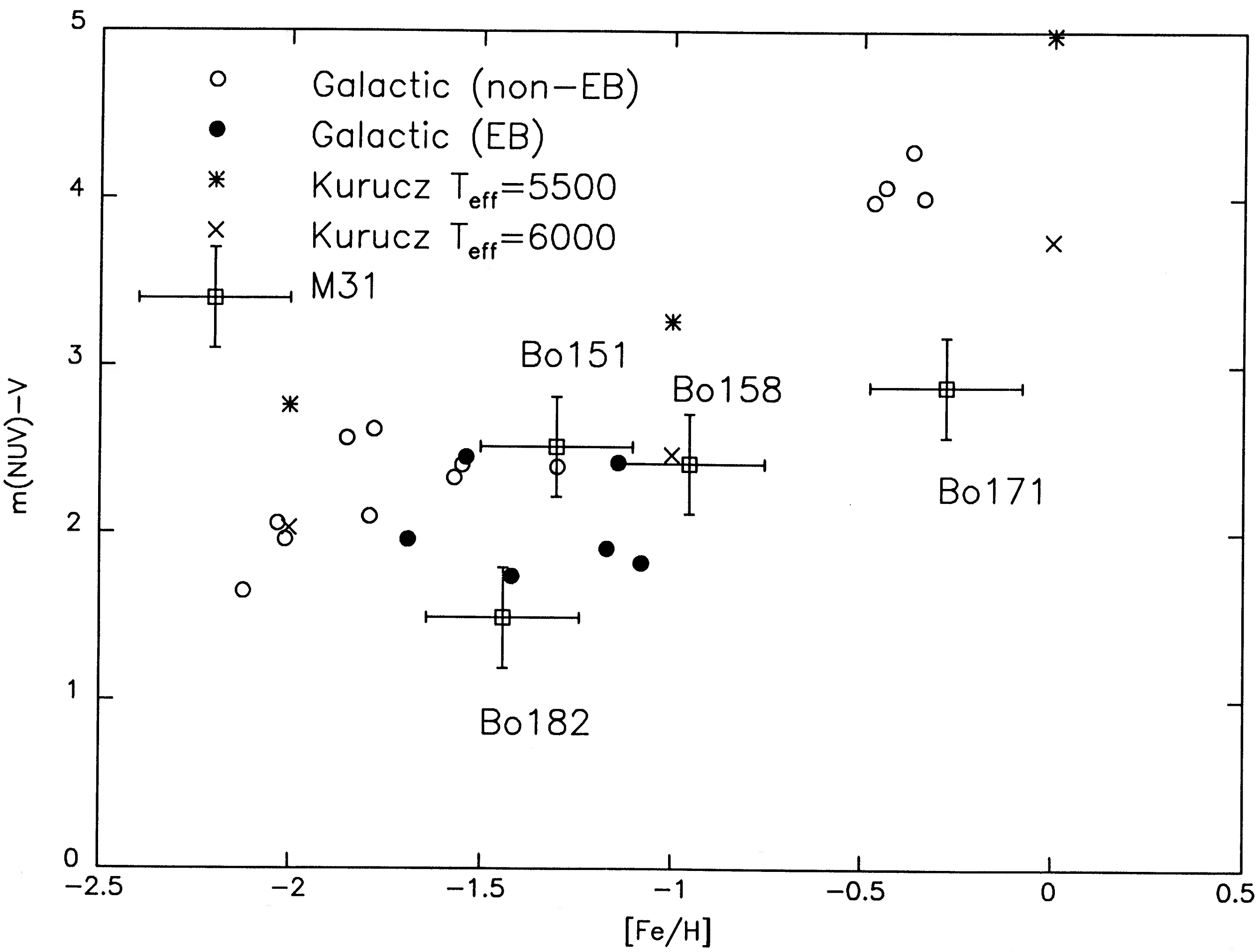

FIG. 4.—Dereddened $m_{NUV} - V$ vs. [Fe/H] for 13 Galactic clusters not classified EB (extremely blue) by van Albada, deBoer, and Dickens (1981), six EB Galactic clusters, and four M31 clusters with visual and UV photometry as in Fig. 1 and [Fe/H] inferred from $V-K$ (Frogel, Persson, and Cohen (1980).

that defined by the Galactic clusters, except for the cluster of highest metallicity, Bo 171, which is ~ 1 mag ($\sim 3\ \sigma$) bluer in $m_{\rm NUV} - V$ than the four Galactic clusters of similar metallicity observed by *ANS*. The four Galactic globular clusters of high metallicity (NGC 104, NGC 6356, NGC 6624, and NGC 6637) have low to moderate reddening, with $E(B-V)$ in the range 0.04–0.25. If the difference in $m_{\rm NUV} - V$ between these Galactic clusters and Bo 171 were caused by reddening, it would imply a difference of ~ 0.2 in $E(B-V)$, which is unlikely. Moreover, contamination of the near-UV flux of Bo 171 is ruled out by the absence of adjacent sources on the M31 atlas print (Hodge 1981). Another possibility is that the metallicity of Bo 171 (computed from $V-K$) has been overestimated, yet the reddening-free Q_K color confirms the high metallicity (Frogel, Persson, and Cohen 1980, citing a private communication of L. Searle). Therefore, the $m_{\rm NUV} - V$ color, although relatively blue considering the observed metallicity, is probably real. It must be due either to a greater number of hot evolved stars or to a younger main sequence than in Galactic globular clusters. If due to the main sequence, the difference in $m_{\rm NUV} - V$ reflects a difference in age distribution between the globular cluster systems of the two galaxies. Very little variance in $m_{\rm NUV} - V$ is evident in Figure 4 within the Galactic sample of high-metallicity clusters, presumably because this sample is uniform in age. The suggestion of younger ages for Bo 158 and Bo 171 is made by Burstein *et al.* (1984), who note the enhanced Hβ and CN line strengths relative to Galactic clusters.

Figure 5 plots $m_{\rm FUV} - V$ versus M_V for the same Galactic and M31 clusters whose $m_{\rm NUV} - V$ colors are plotted in Figure 3, omitting five red Galactic clusters for which no *ANS* 1550 Å magnitudes are available. Limiting colors for M31 clusters are computed from the limiting far-UV magnitudes as described above. The six bluest Galactic clusters in $m_{\rm FUV} - V$ are the six EB clusters. Since essentially all the flux in the 1550 Å band is from the horizontal branch (van Albada, Dickens, and Wevers 1981), this fact is not surprising. The colors of the two reddest M31 clusters detected in the far UV are in the region of the plot occupied by the Galactic EB clusters, as are the limiting colors of the undetected clusters. The three blue clusters detected in the far-UV are discussed in § V.

The limiting values of $m_{\rm FUV} - V$ for Bo 158 and Bo 171 are 1.7 and 1.0, respectively. For Galactic EB clusters, $m_{\rm FUV} - V$

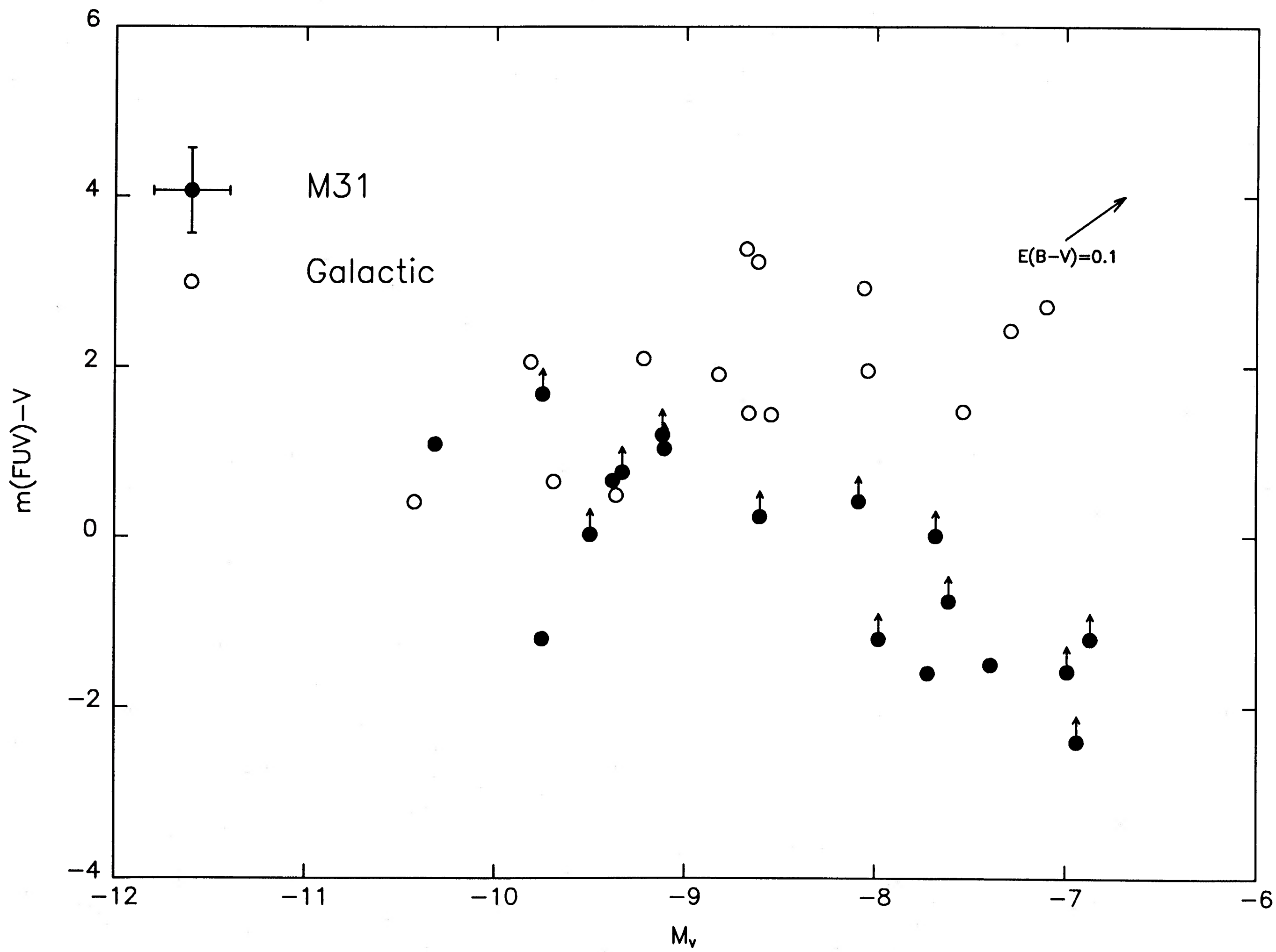

FIG. 5.—Dereddened $M_V - (m_{\rm FUV} - V)$ diagram for M31 and Galactic globular clusters. Solid circles refer to M31 clusters with UV rocket measurements and visual photometry by Battistini *et al.* (1987). The error bar refers to the M31 cluster points. Open circles refer to Galactic clusters with *ANS* 1550 Å band measurements by van Albada, deBoer, and Dickens (1981) and visual magnitudes in an equivalent aperture from Kron and Mayall (1960). The meaning of the arrow is the same as in Fig. 3.

colors computed from *ANS* 1550 Å fluxes are in the range 0.5–1.5. Thus no photometric determination can be made whether either Bo 158 or Bo 171 is of type EB. Nevertheless, for Bo 171, two possibilities can be distinguished. If Bo 171 is not EB, then the near-UV flux must be primarily from the main-sequence turn-off stars, implying a younger age than that of Galactic clusters of similar high metallicity. On the other hand, if Bo 171 is EB, then it is anomalous by Galactic standards in having both high metallicity and an extremely blue horizontal branch, conditions normally considered contradictory.

The case is different for Bo 158, the cluster brightest in the visual of those we detect, with $V = 14.63$ and $m_{\rm NUV} = 17.5$. This cluster was observed with *IUE* by Cacciari *et al.* (1982), who report a flux equivalent to $m_{\rm NUV} = 16.8$, which is 0.7 mag brighter than our point spread function–fit magnitude, but which agrees well with our aperture magnitude (diameter 48″). The additional flux present in our aperture also lies within the *IUE* aperture and is probably associated with a faint, clumpy spiral-arm component visible both in our summed bulge image (Fig. 1) and in the M31 atlas print of the region (Hodge 1981). However, this contamination is outside the image area that is fitted to the PSF, so that PSF fitting is more reliable for this cluster than is aperture photometry. The PSF-fit $m_{\rm NUV}$ determined from the summed bulge image places Bo 158 in a position on the $m_{\rm NUV} - V$ versus M_V diagram (Fig. 3) consistent with other detected M31 clusters of similar V-magnitude. The limiting value for $m_{\rm FUV}$ places Bo 158 in a position on the $m_{\rm FUV} - V$ versus M_V diagram (Fig. 5) consistent with the redder and more metal-rich of the Galactic EB clusters. Cowley and Burstein (1988), who have rereduced archived *IUE* data for Bo 158, obtain a dereddened (2700 − V) color that is consistent with our $m_{\rm NUV} - V$ measurement after correcting for contamination, and they obtain a dereddened (1550 − V) color of 2.03, which is consistent with our $m_{\rm FUV} - V$ lower limit of 1.7.

In addition, Cowley and Burstein (1988) have observed Bo 86 and Bo 206 with *IUE*. They report a (1550 − V) color of 1.09 for Bo 86, consistent with our measurement of 0.7 ± 0.5, but they do not report a far-UV flux or limit for Bo 206. They report (2700 − V) of 1.75 for Bo 86 and 1.83 for Bo 206, consistent with our values of 1.8 and 1.5, respectively.

Bo 338, also observed with *IUE* by Cowley and Burstein (1988), presents another probable case of contamination. Although aperture measurements centered on the position of Bo 338 are consistent with *IUE*, all of these fluxes should be regarded as upper limits because the cluster is located within van den Bergh (1964) association 82, where a high general surface brightness is found in the UV, and where many crowded point sources (probably early-type stars) are found on the M31 atlas print (Hodge 1981). The position of Bo 338 is indicated in Figure 2.

V. BLUE GLOBULAR CLUSTERS IN M31

The four clusters Bo 43, Bo 91, Bo 318, and Bo 327 all have observed $B - V \approx 0.1$–0.3, much bluer than old globular clusters, where $B - V \approx 0.7$–0.9. The corresponding $m_{\rm NUV} - V$ colors (dereddened as discussed below) are roughly −0.6, compared with values greater than 1 for the normal globulars we detect (see Fig. 3). The $m_{\rm FUV} - V$ (similarly dereddened) measurements for Bo 43 and Bo 318 (both −1.5) and lower limits for Bo 91 (−2.4) and Bo 327 (−1.2) are also much bluer than any normal old globular clusters, as plotted in Figure 5. The position of cluster Bo 91 is shown in Figure 1. The positions of the three clusters Bo 43, Bo 318, and Bo 327 are all in the extreme SW arm of M31 and are shown in Figure 2.

Probably, these clusters are compact young clusters similar in age to vdB0, but less massive than vdB0, the position of which is also shown in Figure 2. According to van den Bergh (1969), vdB0 is the most luminous open cluster in M31. Using van den Bergh's *UBV* photometry for vdB0 together with Figure 2 of Searle, Sargent, and Bagnuolo (1973), which gives the locus in the color-color diagram of clusters with a Salpeter initial mass function (IMF) and varying ages, we estimate $E(B-V) = 0.20$. Using the dereddened $B - V$ of ∼0.0 and Table 1 of Searle, Sargent, and Bagnuolo, we estimate an age of $\sim 5 \times 10^7$ yr. The main-sequence turnoff mass is then that mass whose main-sequence lifetime is 5×10^7 yr, or $\sim 5\ M_\odot$ (Iben 1967). Scalo (1986) tabulates main-sequence lifetimes for stars of various masses as determined from models that take convective overshoot into account. The revised lifetime for a $5\ M_\odot$ star is thereby increased to $\sim 1 \times 10^8$ yr, which we adopt as the best estimate for the age of vdB0.

The dereddened $m_{\rm NUV} - V$ and $m_{\rm FUV} - V$ colors of vdB0, computed using $E(B-V) = 0.2$ and the reddening curve of Savage and Mathis (1979), are −0.1 and −1.2, respectively. The stellar UV colors tabulated by Wu *et al.* (1980) are used to compute $m_{\rm NUV} - V$ and $m_{\rm FUV} - V$ for clusters consisting of Salpeter IMFs truncated at various upper mass limits, with all stars having their main-sequence magnitudes. The dereddened $m_{\rm NUV} - V$ for vdB0 is fitted best by the model with upper mass limit at 4.6 $M_\odot$, and $m_{\rm FUV} - V$ is fitted best by a slightly larger mass, $\sim 5.2\ M_\odot$. Given the estimated errors in the observed colors and the approximation that the UV colors can be calculated from a truncated zero-age main-sequence (ZAMS), we consider the agreement with the mass estimate of $5\ M_\odot$ from *UBV* photometry to be satisfactory.

The four blue Bologna clusters have *UBV* colors similar to those of vdB0, and $m_{\rm NUV} - V$ and $m_{\rm FUV} - V$ colors or color limits which are bluer by ∼0.5 mag, probably indicating somewhat lower ages. Turn-off masses are estimated at $\sim 6\ M_\odot$. These clusters are similar in $B - V$, M_V, $m_{\rm NUV} - V$, and $m_{\rm FUV} - V$ to LMC blue globulars of Searle-Wilkinson-Bagnuolo (SWB) type ∼II (Cassatella, Barbero, and Geyer 1987; Searle, Wilkinson, and Bagnuolo 1980), for which Hodge (1983) has estimated ages similar to that obtained for vdB0. (SWB types range from I–VII and increase roughly with cluster age.) The $m_{\rm NUV} - V$ color of Bo 171 (Fig. 4), given the high metallicity, suggests that Bo 171 is intermediate in age between typical Galactic globular clusters and the blue globulars. If so, then M31 has had episodes of globular cluster formation throughout its life, like the LMC and M33 (Cohen, Persson, and Searle 1984). Cowley and Burstein (1988) come to similar conclusions on the existence of intermediate-age clusters in M31 from *IUE* measurements of selected bright clusters. However, since they observe none of the blue globulars, their youngest suggested age of 2×10^9 yr for M31 clusters is still considerably older than the age of $\sim 10^8$ yr for the clusters discussed here.

Figure 6 plots $m_{\rm FUV} - V$ versus $m_{\rm NUV} - V$ for LMC globulars observed by *IUE* (Cassatella, Barbero, and Geyer 1987), Galactic globulars observed by *ANS*, and M31 globulars (blue and red) measured by us. UV fluxes of the LMC globulars are adjusted by −1.0 mag to account roughly for the difference in size between the *IUE* large aperture and the aperture used in the optical photometry. Where possible, LMC clusters are plotted as Arabic numerals giving the SWB type. The relation

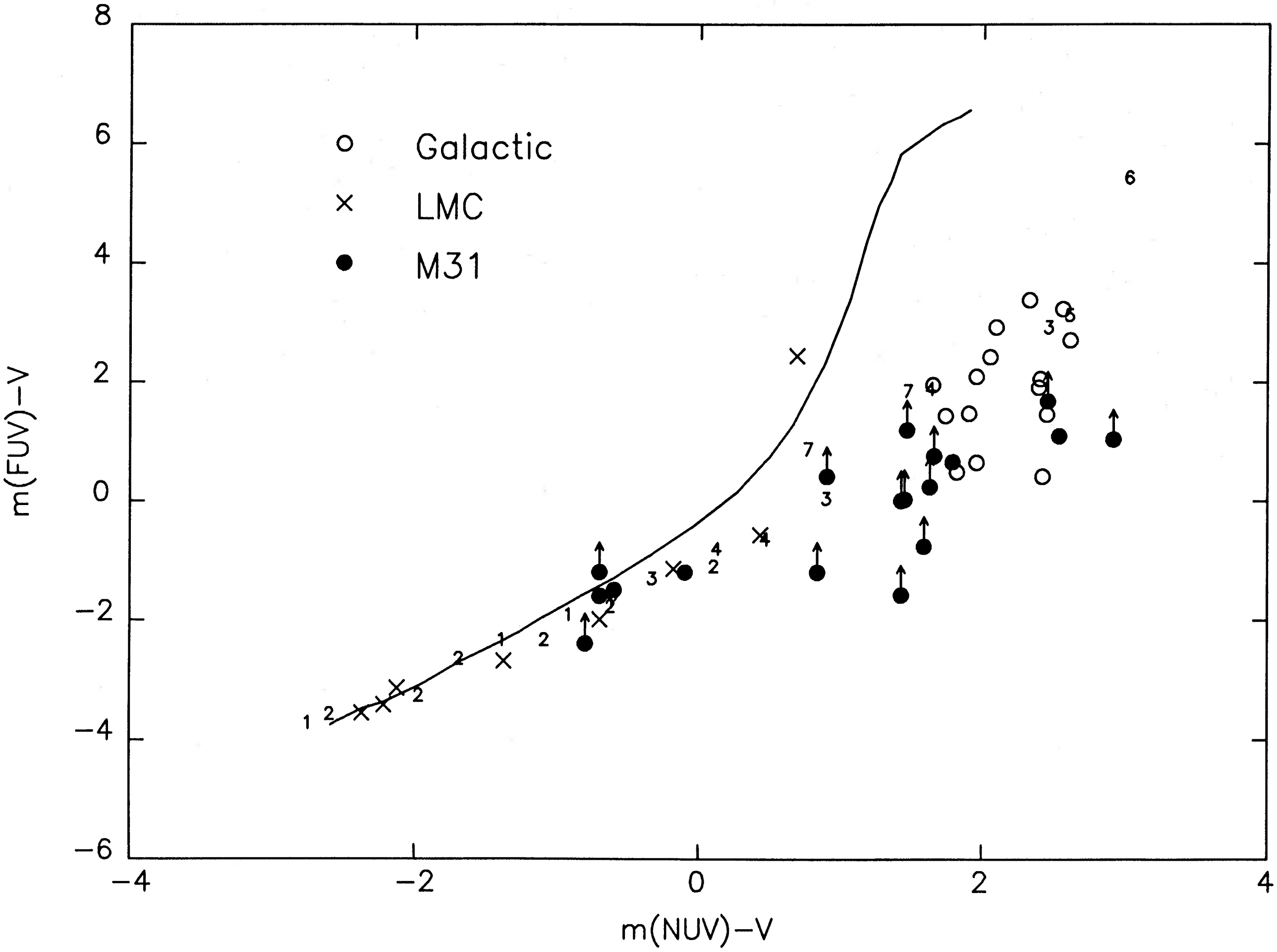

FIG. 6.—Dereddened $m_{FUV} - V$ vs. $m_{NUV} - V$ for LMC globulars (crosses and numbers) as measured by *IUE* (Cassatella *et al.* 1987), Galactic globulars, as measured by *ANS* (*open circles*), and M31 clusters, as measured here (*filled circles*). The numbers indicate the SWB classes (Searle, Wilkinson, and Bagnuolo 1980), for those LMC clusters which have assigned classes. The solid line plots the relation for clusters consisting of a ZAMS with a Salpeter IMF and upper mass limits varying from $\sim 1.5\ M_\odot$ to $\sim 40\ M_\odot$.

between $m_{FUV} - V$ and $m_{NUV} - V$ for our truncated solar-metallicity ZAMS with Salpeter IMF is also plotted. The truncation mass varies from $\sim 1.5\ M_\odot$ at the red end of the line to $\sim 40\ M_\odot$ at the blue end. The LMC globulars span a wide range in $m_{NUV} - V$ and $m_{FUV} - V$, with an approximately linear relation between the two colors. The Galactic clusters occupy the same region of the plot as the redder LMC clusters. The increasing scatter in the distribution of the Galactic clusters as $m_{NUV} - V$ increases is also present in the M31 cluster distribution. The Galactic globulars tend to be redder than the red M31 globulars in $m_{NUV} - V$.

The apparently simple relation between $m_{NUV} - V$ and $m_{FUV} - V$ suggested by the distribution of points in Figure 6 for all three galaxies masks the fact that the evolutionary stage of stars dominating the cluster fluxes changes for the observed bands (visual, near-UV, and far-UV) as $m_{NUV} - V$ increases from -3 to 4. For the bluest clusters, all three bands are dominated by main-sequence stars, the observational scatter is small, and the agreement with the model curve is good. For redder clusters, the visual band is dominated by contributions from the main-sequence and from the early post–main-sequence phases; the far-UV is dominated by the blue horizontal branch; and the near-UV is split between main-sequence turnoff stars and the horizontal branch (with the relative proportions depending on the horizontal branch type). The scatter in the distribution of Galactic clusters is then due to the distribution of metallicities and horizontal branch types. On the other hand, for LMC clusters and M31 clusters, a scatter in ages probably also contributes to the variance in $m_{NUV} - V$.

UIT (§ I) has a higher resolution ($\sim 2''$) and sensitivity than the rocket instrument, and so should be capable of producing magnitudes for most of the Batistini *et al.* cluster candidates in a variety of bandpasses with effective wavelengths ranging from 1400 Å to 2600 Å. Investigations of horizontal branch type, age, and metallicity will then be possible for a large sample of the cluster candidates in M31. The locus in the two-color diagram of Figure 6 occupied by LMC clusters might then be filled in by additional M31 cluster detections. The Bologna cluster list (Battistini *et al.* 1987) contains 16 additional cluster candidates with $B-V < 0.4$, which are either below the detection limit of the sounding-rocket images or outside the imaged fields.

We are grateful to the Sounding Rocket staff at Goddard Space Flight Center for their essential assistance in obtaining the data, to Anne Raugh for assisting in the location of UV sources on the Hodge M31 Atlas prints, and to Barbara Pfarr for assistance with the image processing software. Funding for this project was through NASA Rocket RTOP 879-11-41 and Spacelab Project 440-51-02.

REFERENCES

Baade, W., and Arp, H. 1964, *Ap. J.*, **139**, 1027.
Battistini, P., Bonoli, F., Braccesi, A., Federici, L., Fusi Pecci, F., Marano, B., and Borngen, F. 1987, *Astr. Ap. Suppl.*, **67**, 442.
Bohlin, R. C., Cornett, R. H., Hill, J. K., Hill, R. S., O'Connell, R. W., and Stecher, T. P. 1985*a*, *Ap. J. (Letters)*, **298**, L37.
Bohlin, R. C., Cornett, R. H., Hill, J. K., Smith, A. M., and Stecher, T. P. 1985*b*, *Ap. J.*, **292**, 687.
Bohlin, R. C., Cornett, R. H., Hill, J. K., Smith, A. M., Stecher, T. P., and Sweigart, A. V. 1983, *Ap. J. (Letters)*, **267**, L89.
Bohlin, R. C., Harrington, J. P., and Stecher, T. P. 1982, *Ap. J.*, **252**, 635.
Bohlin, R. C., Hill, J. K., Stecher, T. P., and Witt, A. N. 1982, *Ap. J.*, **255**, 87.
Burstein, D., Faber, S. M., Gaskell, S. M., and Krumm, N. 1984, *Ap. J.*, **287**, 586.
Cacciari, C., Cassatella, A., Bianchi, L., Fusi Pecci, F., and Kron, R. G. 1982, *Ap. J.*, **261**, 77.
Cassatella, A., Barbero, J., and Geyer, E. H. 1987, *Ap. J. Suppl.*, **64**, 83.
Cohen, J. G., Persson, S. E., and Searle, L. 1984, *Ap. J.*, **275**, 92.
Cornett, R. H., Hill, J. K., and Hill, R. S. 1987, *UIT Batch Data Reduction: Data and Programs* (Lanham, MD: ST Systems Corporation; STX-T-25-3002-0007-87).
Courtès, C., Maucherat, J., Monnet, G., Pellet, A., Simien, F., Astier, N., and Viale, A. 1978, *Astr. Ap. Suppl.*, **31**, 439.
Cowley, A. P., and Burstein, D. 1988, *A.J.*, **95**, 1071.
de Vaucouleurs, G. 1978, *Ap. J.*, **223**, 730.
Frogel, J. A., Persson, S. E., and Cohen, J. G. 1980, *Ap. J.*, **240**, 785.
Hill, J. K., Bohlin, R. C., and Stecher, T. P. 1984, *Ap. J.*, **277**, 542.
Hodge, P. W. 1979, *A.J.*, **84**, 744.
———. 1981, *Atlas of the Andromeda Galaxy* (Seattle: University of Washington).
———. 1983, *Ap. J.*, **264**, 470.
Iben, I. Jr. 1967, *Ann. Rev. Astr. Ap.*, **5**, 571.
Kron, G. E., and Mayall, N. U. 1960, *A.J.*, **65**, 581.
Kurucz, R. 1979, *Ap. J. Suppl.*, **40**, 1.
Lasker, B. M., and McLean, B. 1987, private communication.
Pritchet, C. J., and van den Bergh, S. 1987, *Ap. J.*, **316**, 517.
Sargent, W., Kowal, C., Hartwick, D., and van den Bergh, S. 1977, *A.J.*, **82**, 947.
Savage, B. D., and Mathis, J. S. 1979, *Ann. Rev. Astr. Ap.*, **17**, 73.
Scalo, J. M. 1986, *Fundamentals of Cosmic Physics*, **11**, 1.
Searle, L., Sargent, W. L. W., and Bagnuolo, W. G. 1973, *Ap. J.*, **179**, 427.
Sharov, A. S., and Lyuty, V. M. 1983, *Ap. Space Sci.*, **90**, 371.
Stecher, T. P., Bohlin, R. C., O'Connell, R. W., Roberts, M. S., Smith, A. M., and Parise, R. A. 1984, *Bull. AAS*, **16**, 905.
Stetson, P. B. 1987, *Pub. A.S.P.*, **99**, 101.
van Albada, T. S., deBoer, K. S., and Dickens, R. J. 1981, *M.N.R.A.S.*, **195**, 591.
van Albada, T. S., Dickens, R. J., and Wevers, B. M. H. R. 1981, *M.N.R.A.S.*, **196**, 823.
van den Bergh S. 1964, *Ap. J. Suppl.*, **9**, 65.
———. 1969, *Ap. J. Suppl.*, **19**, 145.
Vetesnik, M. 1962, *Bull. Astr. Inst. Czechoslovakia*, **13**, 180.
Welch, G. A., and Code, A. D. 1980, *Ap. J.*, **236**, 798.
Wu, C.-C., Faber, S. M., Gallagher, J. S., Peck, M., and Tinsley, B. M. 1980, *Ap. J.*, **237**, 290.

RALPH C. BOHLIN: Space Telescope Science Institute, Homewood Campus, Baltimore, MD 21218

ROBERT H. CORNETT, JESSE K. HILL, and ROBERT S. HILL: ST Systems Corp., 4400 Forbes Boulevard, Lanham, MD 20706

THEODORE P. STECHER: Code 680, Laboratory for Astronomy and Solar Physics, Goddard Space Flight Center, Greenbelt, MD 20771